EUKARYOTIC CELL, July 2010, p. 1064–1074 Vol. 9, No. 7
1535-9778/10/$12.00 doi:10.1128/EC.00048-10

Systematic Genetic Analysis of the *Plasmodium falciparum* MSP7-Like Family Reveals Differences in Protein Expression, Location, and Importance in Asexual Growth of the Blood-Stage Parasite▽†‡

Madhusudan Kadekoppala,[1]* Solabomi A. Ogun,[1] Steven Howell,[2] Ruwani S. Gunaratne,[1] and Anthony A. Holder[1]*

Divisions of Parasitology[1] and Molecular Structure,[2] MRC National Institute for Medical Research, The Ridgeway, Mill Hill, London NW7 1AA, United Kingdom

Received 24 February 2010/Accepted 10 May 2010

Proteins located on *Plasmodium falciparum* merozoites, the invasive form of the parasite's asexual blood stage, are of considerable interest in vaccine research. Merozoite surface protein 7 (MSP7) forms a complex with MSP1 and is encoded by a member of a multigene family located on chromosome 13. The family codes for MSP7 and five MSP7-related proteins (MSRPs). In the present study, we have investigated the expression and the effect of *msrp* gene deletion at the asexual blood stage. In addition to *msp7*, *msrp2*, *msrp3*, and *msrp5* are transcribed, and mRNA was easily detected by hybridization analysis, whereas mRNA for *msrp1* and *msrp4* could be detected only by reverse transcription (RT)-PCR. Notwithstanding evidence of transcription, antibodies to recombinant MSRPs failed to detect specific proteins, except for antibodies to MSRP2. Sequential proteolytic cleavages of MSRP2 resulted in 28- and 25-kDa forms. However, MSRP2 was absent from merozoites; the 25-kDa MSRP2 protein ($MSRP2_{25}$) was soluble and secreted upon merozoite egress. The *msrp* genes were deleted by targeted disruption in the 3D7 line, leading to ablation of full-length transcripts. MSRP deletion mutants had no detectable phenotype, with growth and invasion characteristics comparable to those of the parental parasite; only the deletion of MSP7 led to a detectable growth phenotype. Thus, within this family some of the genes are transcribed at a significant level in asexual blood stages, but the corresponding proteins may or may not be detectable. Interactions of the expressed proteins with the merozoite also differ. These results highlight the potential for unexpected differences of protein expression levels within gene families.

The human malaria parasite *Plasmodium falciparum* continues to be a major public health challenge mainly in developing countries, claiming more than one million lives annually. The invasion of erythrocytes and the subsequent cycles of growth, replication, and rupture of infected cells are responsible for the primary pathological consequences, such as rapid hemolysis consequent upon merozoite release and metabolic acidosis (17). Therefore, the blood stage of the parasite life cycle is a primary target for interventions to combat malaria disease. Merozoite surface proteins (MSPs) are considered to be among the best candidate antigens for inclusion in an antimalarial vaccine (15, 39). Their surface location implicates these proteins in the initial attachment and invasion of red cells by merozoites and offers good accessibility to host antibodies. Several MSPs are being assessed as vaccine candidates (10, 12, 17, 43).

Merozoite surface protein 1 (MSP1) is located on the developing merozoite surface in association with at least two other proteins—MSP6 and MSP7. Upon invasion of erythrocytes in culture, this protein complex is shed into the supernatant by proteolytic cleavage (3, 4). The complex is comprised of 4 polypeptides generated by sequential proteolytic cleavage of the MSP1 precursor and one polypeptide each from MSP6 (36-kDa protein [$MSP6_{36}$]) (47) and MSP7 ($MSP7_{22}$) (34, 42). Both MSP6 and MSP7 belong to multigene families (29, 36).

The *P. falciparum* MSP7 multigene family comprising *msp7* and five *msp7*-related protein (MSRP) genes is contiguously arrayed on chromosome 13 (11, 29). In rodent malaria parasites *Plasmodium berghei* and *Plasmodium yoelii*, three members, P(b)yMSRP1, P(b)yMSP7, and P(b)yMSRP2, have been identified (29, 34, 45). The predicted proteins are characterized by an N-terminal signal peptide and share greater sequence similarity toward the C terminus. The carboxy-terminal region of MSP7 ($MSP7_{22}$) forms a detergent-resistant complex with MSP1; it is therefore possible that the sequence conservation seen among MSP7-related proteins is essential to their function. The *msp7* gene could be disrupted in both *P. berghei* (45) and *P. falciparum* (19), with apparent but minimal growth consequences. Several MSRPs are expressed in blood stages of *P. falciparum* (6, 22, 23), although their significance to the biology of the parasite is not known. It is often argued that the observed genetic redundancy may translate into functional redundancy. However, there is no direct evidence for any of the MSRPs taking the role of MSP7 in parasites with this gene deleted (19).

The expression of several merozoite proteins has been disrupted by gene knockout strategies (38, 41, 46). While many of

* Corresponding author. Mailing address: Division of Parasitology, MRC National Institute for Medical Research, The Ridgeway, Mill Hill, London NW7 1AA, United Kingdom. Phone: 44 (0) 2088162402. Fax: 44 (0) 2088162730. E-mail for Madhusudan Kadekoppala: mkadeko@nimr.mrc.ac.uk. E-mail for Anthony A. Holder: aholder@nimr.mrc.ac.uk.

† Supplemental material for this article may be found at http://ec.asm.org/.

▽ Published ahead of print on 14 May 2010.

‡ The authors have paid a fee to allow immediate free access to this article.

the glycosylphosphatidylinositol (GPI)-anchored surface proteins were refractory to deletion, disruption of MSP5 (41) and MSP8 (2, 7) was possible but did not result in any measurable change in efficiency of invasion or growth within erythrocytes, demonstrating that the role of each protein is either expendable or can be readily compensated. A more demonstrable compensatory mechanism as a consequence of genetic redundancy, wherein invasion pathways were switched, was reported for gene knockout experiments with proteins such as PfRh1 (46), PfRh2b (1), and erythrocyte binding antigen 175 (EBA175) (8), which are involved in invasion of erythrocytes. Previously, we reported reduced invasion of erythrocytes by the MSP7 deletion in *P. falciparum* parasites (19). In the current investigation, we have examined the expression and the effect of the deletion of *msp7*-related genes. With the antibody reagents developed in the course of this study, we have demonstrated expression and sequential proteolytic processing of PfMSRP2, similar to that previously described for MSP7. Further, PfMSRP2 was found as a soluble protein in the parasitophorous vacuole following recruitment into the secretory pathway. Other MSP7-related proteins, i.e., MSRP1, MSRP3, MSRP4, and MSRP5, were not detected in immunoblots or immunoprecipitates of parasite protein extracts. Also, we report here that the disruption of *msp7*-related genes had no effect on erythrocyte invasion and growth of *P. falciparum*.

MATERIALS AND METHODS

Parasites and transfection. *Plasmodium falciparum* parasites were cultured in RPMI 1640 medium containing Albumax II using human O-positive erythrocytes. The parasite lines used were 3D7 (Netherlands), A4 (Brazil), D10 (Papua New Guinea), FCB1 (Columbia), HB3 (Honduras), T9/96 (Thailand), 7G8 (Thailand), and W7 (Gambia). The trophozoite-schizont–stage parasites were purified by using Percoll gradient centrifugation (35). Merozoites were harvested from magnet-purified schizonts as described previously (5, 44). Ring-stage parasites were transfected with purified plasmid DNA, and drug cycling commenced according to methods described previously (9, 19). The parasites were cultured in a 25-cm^2 culture dish for 48 h prior to selection with 10 nM WR99210. Parasites containing integrated forms of the plasmid were enriched by one or more drug cyclings, in which WR99210 was removed for 2 or 3 weeks before being reapplied. Ganciclovir (10 μM) was added to select for parasites with double recombination at the target gene (9).

Nucleic acid techniques. 5′ and 3′ regions of the target gene open reading frames (ORFs) were cloned on either side of the human dihydrofolate reductase (hDHFR) cassette of the pHTK double recombination construct containing the negative selectable marker thymidine kinase (TK) (9). MSP7-related gene sequences were amplified from *P. falciparum* 3D7 genomic DNA using the oligonucleotides described in Table S2 in the supplemental material. The 5′ PCR product was cloned into a SacII-HpaI (5′-*msrp1*) or SacII-BglII-restricted pHTK plasmid, and ClaI-AvrII-restricted 3′ *msrp1* or EcoRI-AvrII-digested 3′ PCR products of other *msrp* genes were inserted at the corresponding sites of the vector plasmid.

Genomic DNA from parental and cloned transfected parasite lines was isolated by using DNAzol (Invitrogen), and total RNA was purified from late-stage parasites using Trizol (Invitrogen). Southern and Northern hybridization analyses were carried out according to standard protocols. The hybridization probes were prepared by random primer extension of full-length ORFs (19) or 5′ or 3′ regions as described in the figure legends.

Preparation of recombinant MSRPs and antibodies. The 3′ region of the *msrp2* ORF corresponding to amino acids 136 to 281 (MSRP2B) was PCR amplified from the genomic DNA (see Table S1 in the supplemental material) and cloned into pGEX3X (GE Healthcare) to express a glutathione *S*-transferase (GST)-MSRP2B fusion protein in *Escherichia coli* BL21 Gold. The GST tag of the fusion protein was cleaved off with Factor Xa (Roche). The identity of the recombinant protein was confirmed by mass spectrometry-based protein sequencing. Recombinant proteins from the corresponding regions of other MSRPs were prepared as described in the supplemental material. Mouse polyclonal antibodies were raised in BALB/c mice according to standard procedures. Rabbit polyclonal antibodies to the recombinant protein were commercially prepared at Harlan Laboratories. Polyclonal antibodies to MSP7, SERA5, MSP3, and BiP (19) and mouse monoclonal antibody (MAb) 113.1 to MSP2 (13) have been described earlier.

Reverse transcription (RT)-PCR analysis. Total RNA was prepared from Percoll-sorbitol-synchronized 3D7 parasites harvested at 3-h intervals by using Trizol (Invitrogen); residual genomic DNA was removed by DNase I (Invitrogen) treatment and purification on a Mini Elute column (Qiagen). Up to 1 μg of total RNA was used for cDNA synthesis in a reaction volume of 20 μl containing 0.5 μg oligo$(dT)_{15}$ or random primers, 1 mM (each) of the four deoxynucleotides (dNTPs), and 15 units of AMV reverse transcriptase (Promega). Negative controls were set up with equivalent amounts of RNA in the absence of reverse transcriptase. The PCRs were performed with *msrp*-specific primers described elsewhere (19) by using Ampli *Taq* DNA polymerase (Roche Diagnostics GmbH) according to standard procedures. For PF13_0192, oligonucleotides CTCTTAGAATGACGGTACAG and CAAAATCATCATCATCTTCATC were used; *msp1* cDNA was amplified with oligonucleotide pair GATAATATT CATGGTTTCAAATATTTAATTGATGGA and TTCTTTATGTTTTCATTT TTTTTTAAAGTGTCAATACG. Amplified products were visualized by 0.8% agarose gel electrophoresis and ethidium bromide staining.

Parasite extracts, Western blotting, and immunoprecipitation. Percoll-enriched trophozoites and schizonts were lysed in 10 volumes of TEE buffer (50 mM Tris-Cl [pH 7.4], 5 mM EDTA, 5 mM EGTA) and centrifuged at 100,000 × *g* for 30 min at 4°C, and the supernatant was collected as hypotonic lysate. The pellet was sequentially extracted with 10 volumes TEE buffer containing 0.5 M NaCl (salt extract) and then with sodium carbonate buffer (0.1 M, pH 11.0). Time course parasite extracts were obtained from Percoll-sorbitol-synchronized parasites (19). In a separate experiment, late-stage parasites were lysed in 0.15% saponin; soluble and insoluble fractions were collected by centrifugation at 5,000 × *g*. Equal amounts of schizont extracts were resolved in 12% NuPAGE (Invitrogen) and transferred onto Protran (S&S) membrane. Horseradish peroxidase-conjugated anti-mouse or anti-rabbit IgG antibodies (Bio-Rad Laboratories) were used in conjunction with the ECL detection system (Amersham Biosciences, United Kingdom) to visualize antibody reactivity on immunoblots. Immunoprecipitation and detection of ^{35}S-labeled schizont proteins were as described earlier (33).

Immunofluorescence analysis. Formaldehyde-fixed, acetone-permeabilized thin smears of *P. falciparum* 3D7-infected red blood cells (RBC) were incubated with rabbit polyclonal anti-MSRP2B antibodies either alone or together with mouse monoclonal anti-MSP7B antibody (MAb 2G10 generated in the laboratory) for 30 min. Alexa 488- or 594-conjugated secondary antibodies were used to detect binding, and Hoechst 33428 was used to stain parasite nuclei. The images were collected on a Zeiss epifluorescence microscope.

Invasion and growth assay. To determine the growth rate of parasites, the number of infected red cells was counted over a 10-day period by flow cytometry using a fluorescence-activated cell sorter (FACS) as described previously (19, 37), except that hydroethidine (at 50 μg/ml) was used to stain infected RBC (18). The starting parasitemia was ~0.5% with a 2% hematocrit, and the cultures were diluted every 48 h after counting. A total of 100,000 cells were analyzed by the BD CellQuest Pro V5.2.1 software program. Single-cycle assays were performed to determine the rate of invasion in comparison to that of the parental 3D7 line. The results of growth and invasion assays were analyzed by one-way analysis of variance (ANOVA) as described previously (19). Confidence intervals (CI; 95%) for the invasion assay were determined from at least 3 independent experiments, using duplicate cultures of two clones.

RESULTS

Expression of members of the *msp7* locus. Prior to attempting deletion of *msp7*-related genes (*msrp* genes), we wanted to establish transcriptional activity at this locus. Transcription of several members of this gene family has been recorded in the transcriptome (6, 22, 23); the transcripts for *msrp1*, *msrp2*, and *msrp3* have also been detected (29). In this work, oligonucleotide primers designed to amplify the ORFs of *msp7* and *msrp* genes (19) were used in RT-PCR to investigate expression at the *msp7* locus. For *Pf13-0192*, the ORF within the *msrp* cluster coding for a putative transmembrane protein and for *msp1*, located on chromosome 9, primers were designed to amplify

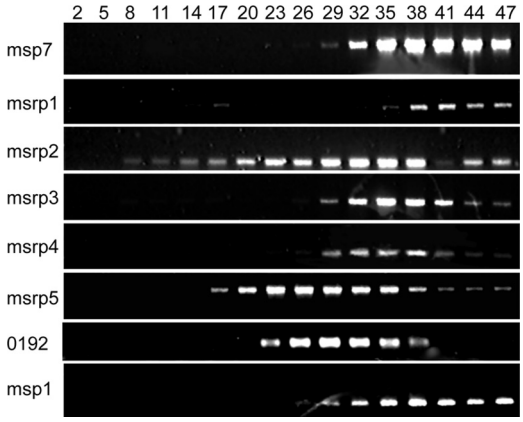

FIG. 1. RT-PCR analysis of *msrp* expression. Total RNA isolated from synchronized 3D7 parasites collected at 3-h intervals (2 to 47 hpi) over one generation was used in a reverse transcription-PCR to amplify *msp7*, *msrp1* to *msrp5*, *PF13_0192* (0192), and *msp1* mRNA.

partial ORFs; *msp1* served as a positive control. Total RNA isolated from Percoll-sorbitol-synchronized parasite culture at 3-h intervals was used for RT-PCR. The RT-PCR analysis presented in Fig. 1 indicates that all members of the *msp7* locus are transcriptionally active. The *msp7* transcription could be detected by 29 h postinvasion (hpi), and the mRNA level increased at later stages. These results agree with earlier reports (34). The *msp1* transcript could be detected by about 26 hpi, and peak steady-state levels of transcript could be detected by about 35 to 38 h. On the other hand, several *msrp* genes were transcribed earlier, though the transcripts could also be detected in late-stage parasites. Minute amounts of *msrp1* transcript were detected in 17-h ring-stage parasites, but the transcript level increased after 35 h, coinciding with schizogony. The immediate downstream gene, *msrp2* was also found to be transcriptionally active in ring-stage parasites at around 8 h. However, the transcript level increased steadily after 17 h and decreased at around 41 h. The transcripts of the *msrp3* and *msrp4* genes were first detected at 29 h, with maximal amounts between 32 and 41 h. On the other hand, *msrp5* gene transcription begins at around 17 h, reaches maximal steady-state levels by 23 to 29 h, and tapers off by 38 h. The unrelated gene within the cluster, PF13_0192, showed transcriptional activity between 23 and 38 hpi. These results are in general agreement with the transcriptome (6, 21), except for *msrp1* and *msrp4*; significant transcript levels for these genes have been detected in this study by RT-PCR.

Expression of MSP7-related proteins. Members of the *msp7* gene family share greater amino acid sequence similarity toward the C terminus; this region of MSP7 is a component of the MSP1 complex located on the merozoite surface, and its absence in an MSP7 deletion mutant of *P. falciparum* produces an invasion phenotype (19). Therefore, carboxy-terminal sequences of MSP7-related proteins were expressed as GST- or six-His fusion proteins and were used to raise mouse and rabbit polyclonal antibodies that were specific for the corresponding protein (see Fig. S1 in the supplemental material). Protein extracts prepared from Percoll-purified trophozoites and schizonts were immunoblotted with anti-MSRP antibodies, since the mRNA for MSP7-related proteins could be detected primarily in these late-stage parasites. Except for the MSRP2B antisera, the antibodies did not react with any specific parasite protein (data not shown). In a dot blot analysis, the recombinant antigens were probed with pooled human serum samples collected from two regions where malaria is endemic, the Gambia and Ivory Coast (data not shown). MSP7 and MSRP2 showed good reactivity with antibodies in the pooled serum samples, and weak but significant reactivity could also be seen with the MSRP3B protein. However, antibodies to MSRP1, MSRP4, and MSRP5 were not detectable in these human antisera.

The immunoblot analysis of 3D7 parasite extracts prepared from synchronized parasites collected at 3-h intervals is presented in Fig. 2A. Rabbit polyclonal antibodies raised against the C-terminal domain of MSRP2 reacted with parasite extracts, detecting 3 protein bands in schizont stages; no reactivity was seen with extracts from ring- and trophozoite-infected (2 to 26 hpi) or uninfected RBC (Fig. 2E). The protein could be first detected 32 hpi as a single band of approximately 35 kDa, even though the mRNA could be detected earlier in ring stages. The electrophoretic mobility of MSRP2 in SDS-PAGE thus agrees with its predicted molecular mass after the removal of the signal sequence (30,365 Da), given its acidic nature (predicted pI of 5.83). The sequential appearance of two more signals in later stages corresponding to 28- and 25-kDa polypeptides suggests that the protein undergoes proteolytic cleavage. However, the 25-kDa species was not always detected by Western blotting of magnet- or Percoll-purified parasites (Fig. 2C). A nonspecific signal corresponding to an 18-kDa protein was also detected in these immunoblots (see Fig. 4C).

Percoll-purified trophozoite/schizont preparations from various laboratory lines of *P. falciparum* were immunoblotted to identify the reactive protein in the parasite extract and to detect patterns of expression of MSRP2. As shown in Fig. 2B, the patterns of reactivity with the MSRP2 precursor and the $MSRP_{28}$ C-terminal region from various laboratory lines of *P. falciparum* were identical. This is unlike the case for MSP7 which showed a clear dimorphism, the presence or absence of $MSP7_{19}$, depending on the presence of a lysine or a glutamine residue at the cleavage site (33).

It is known that the fragments of MSP7, $MSP7_{22}$ and $MSP7_{19}$, are located on the merozoite surface (42) in complex with MSP1 polypeptides and are shed upon invasion of erythrocytes (33, 42). Merozoites released from magnet-purified schizonts in the presence of EGTA retain the MSP1 complex on their surface, owing to the inhibition of MSP1 processing. The protein extract prepared from these merozoites contained both MSP7 forms and MSP3 (Fig. 2C) on Western blots, but MSRP2 was clearly absent from this fraction. Nevertheless, MSRP2, MSP3, and MSP7 could be detected in the culture supernatants collected in the presence or absence of EGTA; MSRP2 was present as $MSRP2_{25}$ in the supernatant, suggesting its formation in mature schizonts or during merozoite release. The BiP protein served as a control for the presence of parasites and was absent in the culture supernatants.

With the immunoblots shown in Fig. 2D and E, the intracellular distribution of PfMSRP2 was investigated by sequential solubility of 3D7 parasite proteins in hypotonic, high-salt, and carbonate buffers or by saponin lysis. The presence of this protein in the soluble fraction suggested no membrane associ-

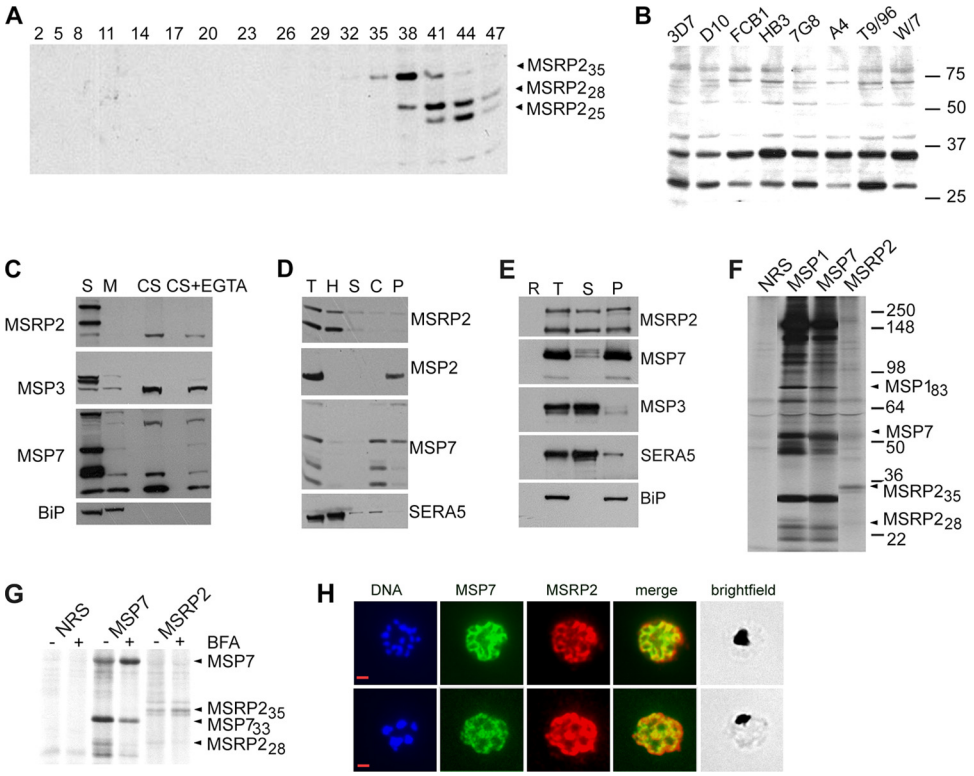

FIG. 2. Expression and distribution of MSRP2. (A) MSRP2 is synthesized late in the cycle and processed; a time course immunoblot analysis of 3D7 parasite extracts is shown. The protein extracts prepared from Percoll-sorbitol-synchronized parasites were electrophoresed on SDS-12% PAGE and probed with rabbit polyclonal anti-MSRP2b antibodies. Molecular weight sizes (in thousands) of the reacting proteins are shown. Hours postinvasion are indicated for each lane. (B) MSRP2 proteins in laboratory parasite lines derived from various geographical isolates have identical patterns of mobility and processing. Protein extracts from Percoll-enriched late-stage parasites were immunoblotted with rabbit polyclonal anti-MSRP2b antibodies. Molecular weight markers (in thousands) are indicated. (C) MSRP2 is present in schizonts but not merozoites, and a processed form is released into culture supernatant. Immunoblot analysis of MSRP2 in trophozoite/schizonts (S), merozoites (M), and culture supernatant (CS). MSP3, MSP7, and BiP antibodies served as control reagents. (D) MSRP2 protein is a soluble protein. Total proteins (T) sequentially extracted by hypotonic- (H), salt-containing (S), and alkaline carbonate (C) buffers or carbonate-insoluble (P) fractions were immunoblotted with MSRP2-, MSP2-, MSP7-, and SERA5-specific antibodies. (E) MSRP2 protein is partially solubilized by saponin treatment. Late-stage parasites were solubilized by saponin; total (T), soluble (S), and insoluble (P) fractions were immunoblotted with MSRP2-, MSP3-, MSP7-, SERA5-, and BiP-specific antibodies. Uninfected RBC (R) extract was included in the blotting. (F and G) Brefeldin A inhibits MSRP2 processing. (F) The immunoprecipitates with antibodies to MSP1, MSP7, and MSRP2 from biosynthetically labeled cultures in the absence of BFA are shown. (G) Magnet-purified *P. falciparum* schizonts radiolabeled in the presence (+) or absence (−) of BFA were solubilized in Nonidet P40-containing buffer, and proteins were immunoprecipitated with either nonimmune rabbit serum (NRS) or rabbit polyclonal antibodies to MSP1, MSP7, and MSRP2. Antigen-antibody complexes were resolved in 8 to 15% SDS-PAGE, and labeled proteins were detected by fluorography. Major immunoprecipitated proteins are marked. Molecular masses of the markers are indicated in kDa. (H) Colocalization of MSP7 and MSRP2. Late-stage parasites were formaldehyde fixed, acetone permeabilized, and reacted with MAb 2G10 (mouse monoclonal anti-MSP7 antibody) and rabbit polyclonal anti-MSRP2 antibodies in an immunofluorescence assay.

ation. Given that there are no transmembrane domains predicted from the sequence, this result indicates that there is also no strong interaction with membrane proteins. In contrast, MSP2, which is a GPI-anchored protein, remained in the carbonate-insoluble fraction. The vacuolar protein SERA5 is released by hypotonic lysis, and PfMSP7 remains insoluble and is extracted by alkaline carbonate buffer. The presence of a small amount of SERA5 in salt- and alkaline carbonate-extractable fractions suggests incomplete solubilization; the same is true for the small amount of MSP7 detected in the carbonate-insoluble fraction. Saponin lysis of late-stage parasites resulted in solubilization of significant amounts of MSRP2, MSP3, and SERA5, whereas most of the MSP7 (associated with parasite membrane) protein remained insoluble (Fig. 2E). BiP also remained in the insoluble fraction. These results together with its solubility in hypotonic buffer (Fig. 2C) suggest that while a significant amount of MSRP2 remains within the parasite, much of it is present as a soluble protein in the parasitophorous vacuole. In immunofluorescence assays conducted upon fixed smears of infected RBC, MSRP2 colocalized with MSP7 (Fig. 2H). The pattern for MSRP2 staining was identical to that of MSP7, except for some regions, generally toward the outside of the infected cell, where MSP7-specific staining could not be detected (Fig. 2H). MSRP2-specific reactivity could not be detected in ring or trophozoite stages and merozoites (data not shown).

The immunoprecipitation of parasite proteins or protein complexes reacting with polyclonal anti-MSRP2 antibodies is presented in Fig. 2F and G. Mouse MAb 12.8 to MSP1$_{19}$ and rabbit polyclonal antibodies to MSP7 were used as controls.

Both these antibodies produced the expected identical patterns corresponding to the MSP1 complex (Fig. 2F). On the other hand, two specific proteins, indicated as $MSRP2_{35}$ and $MSRP2_{28}$, were immunoprecipitated by the polyclonal antibodies to MSRP2. In order to examine whether the proteolytic cleavage occurs in a post-Golgi compartment, brefeldin A (BFA) was used to block transport of ^{35}S-labeled proteins in *P. falciparum*. It is known that BFA-mediated blocking of protein transport also leads to accumulation of MSP1 and MSP7 precursors within the parasite as a binary complex (33). The results presented in Fig. 2G revealed effective blocking of the proteolytic processing of MSRP2 by BFA, indicating that this proteolysis occurs in a post-Golgi compartment of the parasite. As a result, BFA treatment leads to accumulation of an MSRP2 precursor ($MSRP2_{35}$), but unlike MSP7, the immunoprecipitated MSRP2 did not have bound MSP1 polypeptides. In the reciprocal immunoprecipitation assay with MSP1-specific antibodies, MSRP2 was not detected (Fig. 2F).

Disruption of MSP7-related genes. To determine whether or not MSP7-related proteins perform a function essential to the erythrocytic cycle, we attempted to disrupt members of the *msp7* gene family. The transfection plasmids were designed to insert a human DHFR (WR99210-resistant) cassette by double homologous recombination at the target locus, thereby abolishing synthesis of a functional mRNA. The parental 3D7 and altered physical map of the *msp7* locus in the gene disruption parasites is presented in Fig. 3A. As described above in "Nucleic acid techniques," 5′ and 3′ regions of the ORFs were cloned into the negative selection plasmid pHTK (9). Upon transfection of these plasmids individually into *P. falciparum* 3D7, WR99210-resistant parasites appeared after 3 or 4 weeks and were then subjected to drug cycling and negative selection with ganciclovir. The transfected populations were cloned, and randomly selected clones from each transfection were analyzed. Southern blot analyses of restricted genomic DNA from two representative clones (Fig. 3B to G) showed that the plasmids had integrated into the target site via the expected recombination events. In Southern analysis of 3D7 Δ*msrp1* parasite genomic DNA restricted with EcoRI, 5′-*msrp1* and 3′-*msrp1* probes hybridized with 6.4-kb and 0.5-kb DNA fragments, respectively (Fig. 3B). This pattern is distinct from a single 4.8-kb signal seen with 3D7 genomic DNA and supports the observation that the *msrp1* gene is disrupted. Genomic DNA restricted with EcoRI and hybridized with *msrp3*-derived probes displayed a single 9.0-kb DNA fragment (Fig. 3C). On the other hand, a 5′-*msrp3* probe hybridized to a 4.0-kb fragment and a 3′-*msrp3* probe hybridized to a 7.0-kb DNA fragment (Fig. 3C). Similarly, *msrp4*- and *msrp5*-derived probes detect a single 6.4-kb DNA fragment in 3D7 genomic DNA restricted with XbaI but reveal two distinct DNA fragments in respective knockout parasites (Fig. 3D and F). The *msrp4* locus in the 3D7 Δ*msrp4* parasite is disrupted to yield 2.5-kb and 4.8-kb fragments that hybridized with 5′ *msrp4* and 3′-*msrp4* DNA probes (Fig. 3D). In 3D7 Δ*msrp5* parasites, the 5′-*msrp5* probe detected a 4.0-kb signal, whereas the 3′-*msrp5* probe detected a 2.4-kb DNA fragment. All these results were consistent with the predicted hybridization patterns.

Whereas disrupted loci of other *msp7*-related genes could be detected by genomic hybridization techniques following ganciclovir selection after one or two drug-cycling steps (removal and reintroduction of WR99210), the attempts to disrupt the *msrp2* gene were not as successful. For reasons not known, ganciclovir selection did not yield parasites with *msrp2* disrupted by double recombination (data not shown). Nevertheless, parasites carrying integrated plasmids were enriched after 4 drug cycles spread over more than 9 months. These parasites were cloned; analysis of two representative clones revealed integration of a single copy of the plasmid by recombination via 5′ *msrp2*. As shown in Fig. 3G, *msrp2*-derived probes detected a single 5.1-kb signal in BglII-restricted 3D7 genomic DNA, which in 3D7 Δ*msrp2* is replaced by two DNA fragments of 3.2 and 10.5 kb detected by a 5′-*msrp2* probe and a single 10.5-kb fragment detected by a 3′-*msrp2* probe. The 10.5-kb DNA fragment hybridizing to both 5′- and 3′-*msrp2* probes was the result of duplication of the 5′-*msrp2* region due to integration of the episome via the 5′-*msrp2* region of the plasmid construct, as shown in Fig. 3A. Therefore, two signals were detected with the 5′-*msrp2* probe. The single 10.5-kb DNA fragment seen with the 3′-*msrp2* probe confirmed the absence of recombination in the 3′ region, since a 4.2-kb signal would have resulted from double recombination. Hybridization analysis with both *msrp2*-derived probes detected a single 14.0-kb signal in PacI-restricted genomic DNA of 3D7 Δ*msrp2* parasites (data not shown), further evidence for the integration of the 8.5-kb transfection plasmid, which lacks a PacI site.

We also attempted to delete all members of the *msp7* gene family (using a pHTK plasmid carrying 5′-*msp7* and 3′-*msrp5* regions), *msrp1* to *msrp5* (a plasmid construct carrying 5′-*msrp1* and 3′-*msrp5* regions), or two adjacent genes simultaneously. Of these transfection experiments, only one, in which both the *msrp3* and *msrp4* genes were deleted, was successful. As shown in Fig. 3E, a 9.0-kb signal seen with EcoRI-restricted 3D7 genomic DNA is absent in the 3D7 Δ*msrp3-4* parasite. This knockout parasite contained an altered locus, with two DNA fragments detected: 4.0 kb and 1.5 kb detected by 5′-*msrp3* and 3′-*msrp4* probes, respectively. As can be seen from the map of the *msp7* locus (Fig. 3A), this disruption of *msrp3* and *msrp4* also deletes PF013_0192, a gene that shares no significant similarity to MSP7-related genes.

To examine transcription at the *msp7* cluster in wild-type and mutant parasites, total RNA isolated from the parental 3D7 and two cloned lines from each knockout was analyzed by Northern blotting. The results are presented in Fig. 4A; calmodulin mRNA was used as a control. The *msp7* and *cam* transcripts were detected in all the parasite lines tested. In wild-type parasites, transcripts for *msrp2*, *msrp3*, and *msrp5* were detected; mRNA for *msrp1* and *msrp4* was not detectable. On the other hand, parasites in which particular *msrp* genes were disrupted did not produce the corresponding transcript. Thus, insertion of the hDHFR cassette abolished transcription of the targeted *msrp* gene. A small amount of longer or shorter transcripts was seen with Δ*msrp2* and Δ*msrp5* mutant parasites (Fig. 4A); these could be due to low transcription of the 5′-*msrp2* or 5′-*msrp5* region, which retains the necessary 5′-untranslated region (UTR) promoter regions but lacks 3′-UTR transcription terminator sequences.

In the Northern analysis (Fig. 4A), whole ORFs of *msrp* genes were used as probes. Although no signals corresponding to the full-length or truncated transcript could be seen, the more sensitive RT-PCR method of analysis was used to further

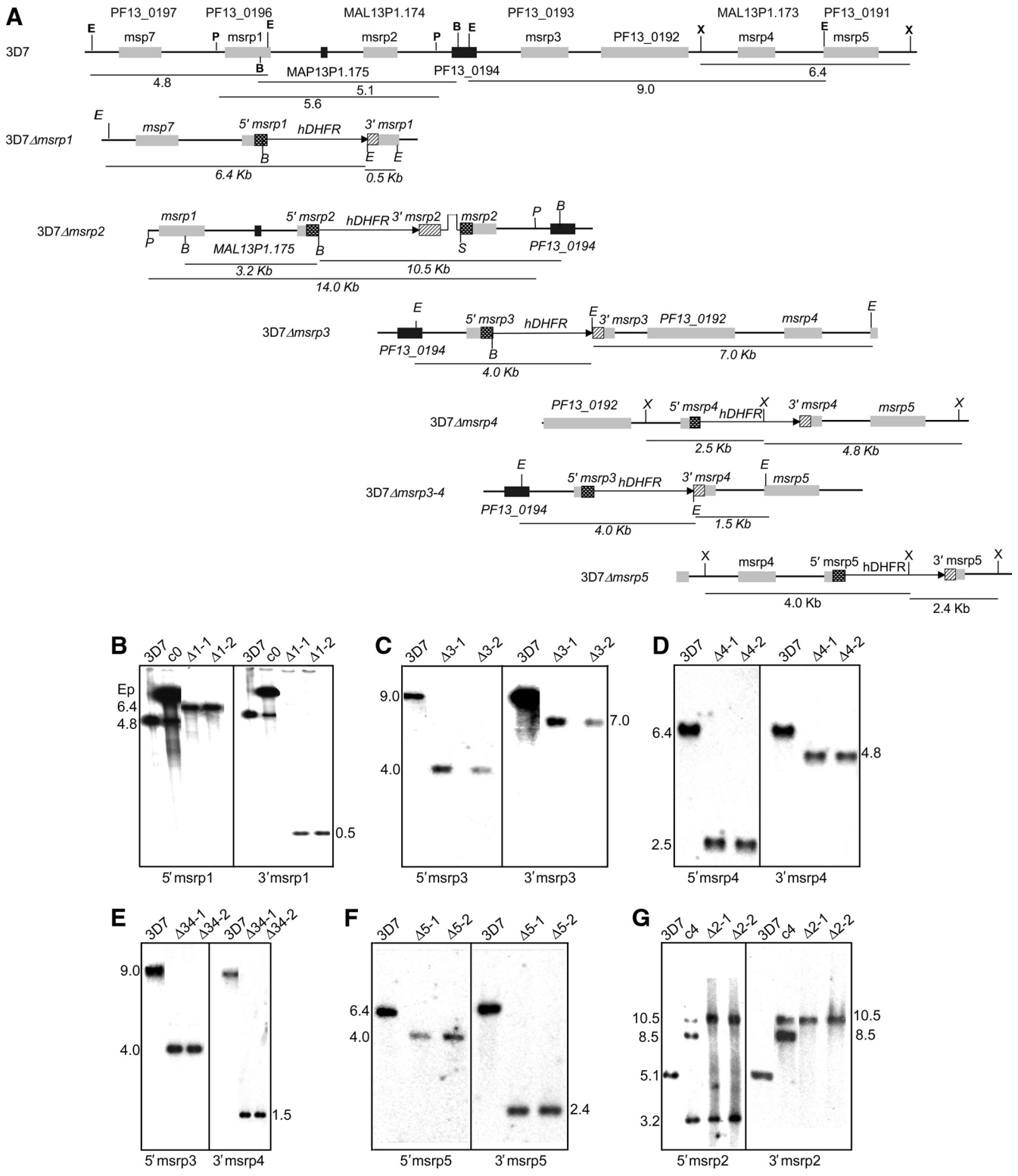

FIG. 3. (A) Schematic of the *msp7* gene family locus of *P. falciparum* 3D7 and knockout parasites. Nomenclature of MSP7-related genes is adapted from reference 29. Pseudogenes (black boxes) and the unrelated gene PF13_0192 are also shown. Gray boxes represent parental ORFs, and checkered and hashed boxes are from the transfecting plasmid. Human DHFR cassette is indicated by an arrow. Relevant restriction sites used in this investigation are marked (B, BglII; E, EcoRI; P, PacI; S, SacII; X, XbaI). DNA fragments generated in the Southern analysis are shown as lines below or above the physical map, with molecular masses indicated. (B to G) Southern hybridization analysis of genomic DNA from parental 3D7 and knockout parasites. Molecular weight sizes (in thousands) of the hybridizing restriction fragment of the resident locus, episome (Ep), and altered locus in the knockout parasites are marked. Hybridization probes are indicated below each panel. In panels B to F, EcoRI-restricted genomic DNA from 3D7 and transfected parasites (c0 for 3D7 Δ*msrp1*), two clones each from 3D7 Δ*msrp1* (Δ1–1 and Δ1–2), 3D7 Δ*msrp3* (Δ3–1 and Δ3–2), and 3D7 Δ*msrp3*-4 (Δ34–1 and Δ34–2) probed with 5′- and 3′-gene-specific DNA probes. For clones of 3D7 Δ*msrp4* (Δ4–1 and Δ4–2) and 3D7 Δ*msrp5* (Δ5–1 and Δ5–2) parasites, XbaI-restricted genomic DNA was used. In panel G, genomic DNA from 3D7 parasites, transfected parasites after 4 drug cyclings (c4), and two clones of 3D7 Δ*msrp2* (Δ2–1 and Δ2- 2) restricted with BglII and hybridized with 5′-*msrp2* and 3′-*msrp2* DNA probes.

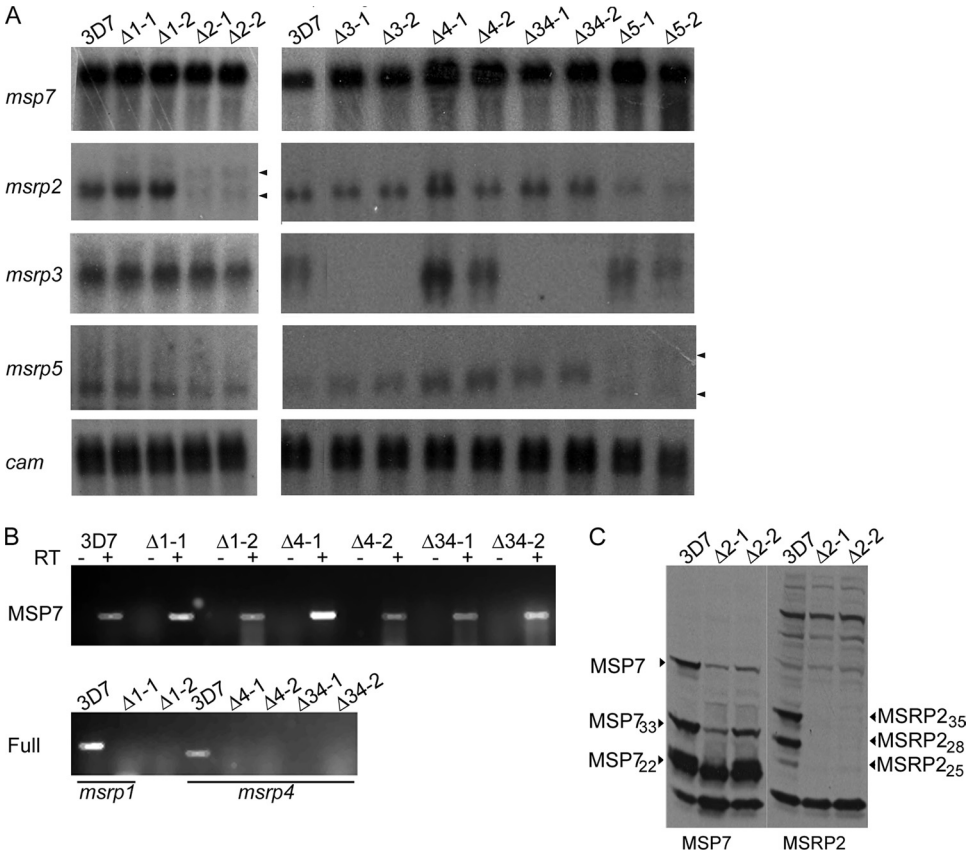

FIG. 4. Analysis of transcription of targeted genes. (A) Up to 3 μg of total RNA from parental line and two clones each from transfectant lines were hybridized with PCR-amplified ORFs of *msp7*, *msrp2*, *msrp3*, and *msrp5*. Calmodulin (*cam*) was used as a distant locus control for transcription. Weak nonspecific signals in 3D7 Δ*msrp2* and 3D7 Δ*msrp5* lanes are indicated by arrowheads. (B) cDNA synthesized from total RNA by priming with random hexamers was used to amplify *msp7*, *msrp1*, and *msrp*4 from parental and genetic deletion clones. Amplification of MSP7 in the presence (+) or absence (−) of reverse transcriptase (RT) served as a control. Lanes for 3D7 and deletion mutants are labeled as described in the legend for Fig. 3B to G. (C) Immunoblot analysis of protein extracts from parental (3D7) and *msrp2* deletion clones (Δ2–1 and Δ2–2) with rabbit polyclonal antibodies to MSP7 and MSRP2B. Different forms of MSP7 and MSRP2 are identified. The precursor and proteolytic products of MSRP2 are absent in the deletion clones.

support this observation and to analyze *msrp1* and *msrp4*, the transcripts of which were not detected in total RNA by Northern hybridization. cDNA was prepared from total RNA by using random decaprimers and gene-specific primers for full-length and 5′ or 3′ regions of *msrp* genes were used to PCR amplify *msp7* and *msrp* genes. The *msp7* mRNA was detected in all the parasite lines (Fig. 4B). As seen in the figure, the knockout parasites did not show any full-length transcripts of *msrp1* and *msrp4*. A similar result was also obtained by applying the same approach to *msrp2*, *msrp3*, and *msrp5* (see Fig. S2 in the supplemental material).

To examine the expression of MSRP2 in the wild-type and *msrp2* knockout parasite populations, extracts of late-stage parasites from the parental and Δ*msrp2* mutant clones were collected and analyzed by Western blotting. Anti-MSP7 antibodies detected precursor 33- and 22-kDa species of MSP7 in both the parental and MSRP2-disrupted parasite lines (Fig. 4C, left). In contrast, anti-MSRP2 antibodies reacted with the expected 35- and 28-kDa species exclusively in the parental parasite line but did not detect these forms in the *msrp2*-disrupted line (Fig. 4C, right). In addition to several large proteins (>45 kDa), an 18-kDa polypeptide cross-reacting with anti-MSRP2 antiserum was present in both the wild-type and the Δ*msrp2* mutant parasite protein extracts. Since the *msrp2* transcript was not detected, this 18-kDa signal could not be due to a truncated form of MSRP2. Presumably, this protein must share epitopes with MSRP2; it was also seen in extracts prepared from D10ΔMSP7 and other MSRP deletion mutants of 3D7 (data not shown).

Loss of MSRP expression does not affect red blood cell invasion or blood-stage-parasite growth rates. The absence of detectable MSRP2 on the surface of invading merozoites suggests that this protein may not play a role in erythrocyte invasion. As described above, the expression and location of other MSRP proteins could not be clearly demonstrated. Nevertheless, the deletion mutants were tested in erythrocyte invasion and growth assays in comparison with the parental 3D7 parasite. Rates of invasion were averaged from the results of at least three independent single-cycle invasion assays, and the 95% CI was calculated for each deletion mutant (Fig. 5A). The loss of MSRP expression did not affect erythrocyte invasion, as the parental 3D7 and ΔMSRP mutant parasite lines were indistinguishable ($P > 0.05$) in their ability to invade erythrocytes.

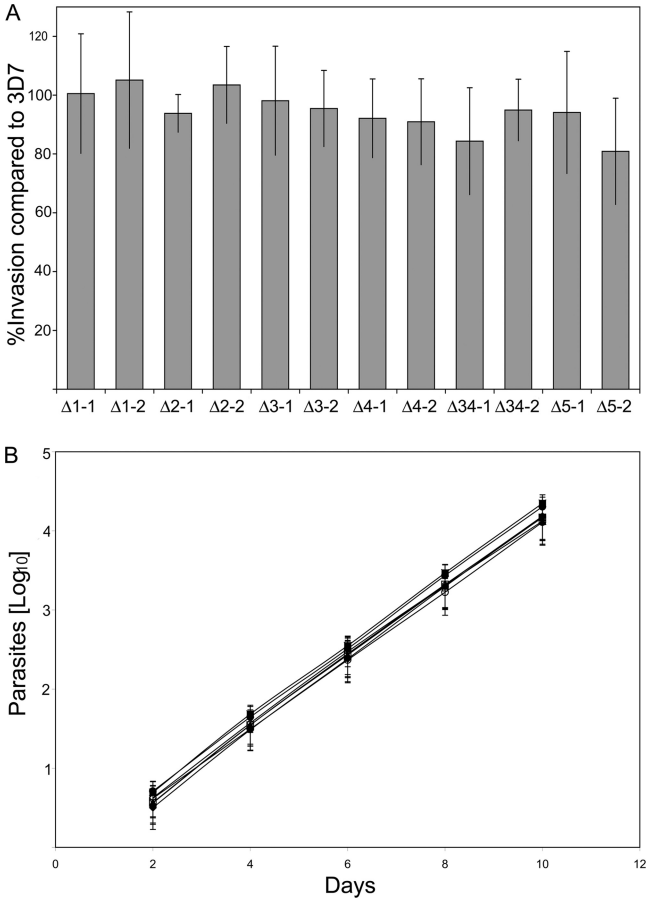

FIG. 5. Invasion and growth of deletion mutant parasite lines. (A) Single-cycle invasion assay of 3D7 and disruption mutants 3D7 Δ*msrp1* (Δ1–1, Δ1–2), 3D7 Δ*msrp2* (Δ2–1, Δ2–2), 3D7 Δ*msrp3* (Δ3–1, Δ3–2), 3D7 Δ*msrp4* (Δ4–1, Δ4–2), 3D7 Δ*msrp3-4* (Δ34–1, Δ34–2), and 3D7 Δ*msrp5* (Δ5–1, Δ5–2). The mean parasitemia compared to that of parental 3D7 parasites from three independent assays is presented. Error bars represent 95% CI. (B) Growth of parental (3D7, ■) and cloned transfectant lines (3D7 Δ*msrp1*, ●; 3D7 Δ*msrp2*, ○; 3D7 Δ*msrp3*, ▲; 3D7 Δ*msrp4*, ◆; 3D7 Δ*msrp3-4*, □; 3D7 Δ*msrp5*, ◇) over a 10-day period. Each point corresponds to mean parasitemia of two individual clones cultured in duplicates with 95% CI as error bars. Parasitemia was determined by FACS analysis of hydroethidine-labeled parasites. The results indicated that the knockout parasite lines grew at the same rate as 3D7 *in vitro* ($P > 0.05$).

The *in vitro* growth rates of the parental 3D7 parasites and two cloned lines from each deletion mutant were compared over 10 days under standard culture conditions. The parasites were synchronized at ring stages, and parasitemia was determined by a FACS-based assay. As shown in Fig. 5B, no significant difference ($P > 0.05$) between the growth rates of the parental and cloned *msrp* deletion lines was observed. Thus, there was no consistent effect on ability to invade and grow within erythrocytes as a consequence of disruptions of *msp7*-related genes.

DISCUSSION

In this paper, we describe the successful disruption of genes encoding five MSP7-related proteins of *P. falciparum*. Four of these genes could be disrupted by double recombination, leading to insertion of the hDHFR cassette of the transfecting plasmid, whereas single-site integration of the episome was observed at the *msrp2* locus, effectively disrupting transcription of full-length mRNA. However, our investigation of the expression and significance of MSP7-related proteins has not yielded clear results relating to a function. Although antibodies developed against recombinant antigens showed no significant cross-reactivity with other MSP7 family members on immunoblots of recombinant proteins, many of these antibody reagents did not react with the corresponding specific proteins on immunoblots of parasite extracts. However, anti-MSRP2 antibodies reacted with two major parasite proteins of 35 and 28 kDa. As the predicted molecular mass of MSRP2 is 30.8 kDa, it is likely that the 35-kDa protein ($MSRP2_{35}$) represents the full-length MSRP2. We propose that the 28-kDa species ($MSRP2_{28}$) is likely to be a C-terminal fragment analogous to $MSP7_{22}$. The initial appearance of a single 35-kDa band which diminishes in time with the gradual increase in 28-kDa and later 25-kDa signals on the time course immunoblots is consistent with this precursor-product relationship. The 25-kDa form was not always seen with protein extracts prepared from parasites but was abundant in culture supernatant. Therefore, it is likely that the secondary cleavage occurred at the time of merozoite egress. Proteolytic processing is a feature common to many merozoite surface and parasitophorous vacuolar proteins that have been characterized. These sites have been identified as recognition and cleavage sites for the subtilisin-like enzyme SUB1, and a consensus recognition sequence has been deduced (20). The cleavage site in MSRP2 has not been identified experimentally, but it is possible that SUB1 may be responsible for the cleavage. Two potential cleavage sites (indicated by ¡ in sequences), within ^{90}SLKGE¡SEDNT^{99} and ^{105}KVQGA¡qVDqA^{114} conforming to the consensus SUB1 recognition sequence (20), are present in MSRP2. The prediction of the latter site is less strong, owing to two glutamine residues (shown in lowercase), which are not present at the positions in the consensus recognition sequence reported by Koussis et al. (20). However, it should be noted that the SUB1 protease displays significant flexibility, and therefore, this protease may be responsible for both of the proteolytic events resulting in $MSRP2_{25}$. Also, the small difference observed in the apparent mass of the two processed forms seems to agree with the 15-amino acid residue separation between the two predicted SUB1 sites. On the other hand, given the temporal separation of the two MSRP2 proteolytic processing events, it is likely that different proteases are involved. *In vitro* experiments with recombinant PfSUB1 have shown PfSUB1-mediated cleavage of the parasite-derived MSRP2 precursor to the 25-kDa form (Natalie Silmon de Monerri and Michael Blackman, personal communication).

Transcripts for several *msrp* genes could be detected by RT-PCR and Northern hybridization analysis. Though transcripts for *msrp1* and *msrp4* were detected by RT-PCR, Northern analysis did not yield any detectable signal in repeated experiments with RNA from the 3D7 parasite line. This is also in agreement with data recorded in the *P. falciparum* transcriptome (6, 21, 23), where sorbitol-synchronized 3D7 parasites showed very low levels of *msrp1* and *msrp4* transcripts. On the other hand, *msrp1* and *msrp4* transcripts could be detected in

late stages of the D10 parasite line, albeit at low levels compared to other *msrp* genes (19). However, significant amounts of *msrp1* transcript were detected by Mello et al. (29), and MSRP1 was reported to be present in the detergent-resistant membrane fraction (40). Recent comparative transcriptome analyses (25) indicate strain differences in the transcription of a given gene and significant downregulation of *msrp1* transcript in the field isolates of *P. falciparum* parasites, and this phenomenon may explain some of these different findings. Notwithstanding the presence of detectable transcript levels for *msrp3* and *msrp5*, the corresponding proteins could not be detected using antibody reagents developed in this study. Such anomalies may be quite common; the absence of mRNA-to-protein correlation has been reported for *P. falciparum* (21) and *P. berghei* (16) in addition to a posttranscriptional gene silencing mechanism in the latter species (27).

Results from RNA and protein expression analysis, together with cellular localization studies, demonstrate that MSRP2 is expressed in the asexual erythrocytic stage of parasite development. This is in agreement with its identification in the parasite proteome (21) and the presence of antibodies in the sera of populations in the Gambia and the Ivory Coast where malaria is endemic (data not shown). In contrast, these serum samples were negative for antibody reactivity to other recombinant MSRPs, except for weak reactivity to MSRP3. The presence of MSRP2 protein in parasite isolates from various geographical locations suggests an important role for this protein. Unlike MSP7 (33), the MSRP2 proteins appeared to be identical in size among these isolates as determined by immunoblotting. Further, the results presented here show that MSRP2 is a soluble protein located in the parasitophorous vacuole, very much unlike MSP7, which is associated with the membrane through MSP1 via detergent-resistant noncovalent interactions. Although MSRP2 is present in the late stages of the erythrocytic life cycle, merozoites were devoid of any detectable protein.

Antibodies affinity purified with MSRP3b, MSRP4b, and MSRP5b recombinant proteins did not recognize specific parasite proteins. Whereas anti-MSRP1b, anti-MSRP3b, and anti-MSRP4b antibodies did not react with any parasite protein, anti-MSRP5b antibodies reacted with several polypeptides (data not shown). It is likely that owing to their less-abundant transcripts, MSRP1 and MSRP4 are not expressed as proteins in the erythrocytic stages of 3D7 parasites. However, their expression remains to be investigated in greater detail, and the presence of any of the proteins at a low level cannot be ruled out. The antigen specificity of these antibodies for MSRPs (except for MSRP2) could not be validated by using the gene disruption mutants generated in this study.

It is generally believed that the multigene families arose due to tandem amplification that provides genetic and functional redundancy. The numerical difference in MSP7 gene family members among different species of *Plasmodium* is noteworthy. The rodent malaria parasites *P. berghei*, *P. chabaudi*, and *P. yoelii* have three members each. *P. falciparum* has 8 members (including two pseudogenes), whereas another human parasite, *P. vivax*, has at least 11 MSP7-like genes in the syntenic region of chromosome 13 (31). In the syntenic region of chromosome 12 of the primate malaria parasite, *P. knowlesi*, at least 4 MSP7-like genes have been identified. In the current investigation, we have shown that only MSRP2 protein is expressed (in addition to MSP7) in the asexual blood stages of laboratory lines of *P. falciparum*. On the other hand, all three members are expressed in *P. yoelii* (28, 29; unpublished data). The significance of the differing sizes of the MSP7 gene family among malaria parasites and the physiological role of the gene products remain elusive.

Genomic integration of plasmid DNA occurs inefficiently in *P. falciparum*, as it is restricted mainly to homologous regions. The targeted disruption of genes in families encoding proteins located on the merozoite surface or in the apical organelles has identified a significant degree of functional redundancy. For example, the paralogues EBA175, EBA181, and EBA140 have different binding specificities for red cell surface proteins, and as a consequence, parasites with genetic disruption in individual EBAs remain viable *in vitro* (14, 26, 38) by the switching invasion pathway. In these cases, the phenotypic consequences of genetic deletion were readily detectable under culture conditions. Notwithstanding the absence of an observable phenotype, a similar situation may still apply to MSP7-related proteins in which paralogues provide duplication or overlapping function and consequently the deletion mutants have no observable phenotype. No detectable growth phenotype was reported for deletions of *msp5*, *msp3*, and *msp6*, yet the genes for these proteins along with MSP7 are retained by parasites in natural infections, as can be deduced from reports of antibodies in serum samples collected from individuals living in areas where malaria might be endemic (48). Except for MSRP2, the knockout of MSRP genes was achieved with relative ease. However, the episome integration at the *msrp2* locus ablated synthesis of full-length mRNA and the MSRP2 protein. The ability to genetically disrupt MSRP2 and other MSRP gene products without any significant phenotype, in contrast to the invasion phenotype observed with genetic deletion of MSP7, suggests that MSRPs either play a minor role in blood-stage parasites or are functionally redundant. The rodent parasite orthologue PyMSRP2 has been shown to confer immunity to *P. yoelii* blood-stage infection in mice (28). However, PyMSRP2 could be detected on the merozoite surface, unlike its orthologue in *P. falciparum*. In single-cycle invasion assays, polyclonal antibodies to MSRP2B did not affect growth of *P. falciparum* (data not shown). Whether the susceptibility or refractoriness to genetic deletion of a gene for a malaria protein in laboratory cultures reflects its utility as a vaccine candidate is matter of considerable interest. Despite the fact that deletion or truncation of MSP3 (30; Ellen Knuepfer, personal communication) did not affect the parasite's ability to invade and develop within erythrocytes, MSP3 is being evaluated for its vaccine potential (24, 32). However, the absence of MSRP2 on *P. falciparum* merozoites may rule out the consideration and use of this protein as a vaccine candidate.

ACKNOWLEDGMENTS

We thank Munira Grainger for assistance with parasite culture and Brendan S. Crabb for critical reading of the manuscript.

This work was supported by the United Kingdom Medical Research Council (U117532067), the U.S. National Institutes of Health (HL078826), the European Union through the BioMalPar Network of Excellence, and the U.S. Agency for International Development.

REFERENCES

1. **Baum, J., A. G. Maier, R. T. Good, K. M. Simpson, and A. F. Cowman.** 2005. Invasion by *P. falciparum* merozoites suggests a hierarchy of molecular interactions. PLoS Pathog. **1:**e37.
2. **Black, C. G., T. Wu, L. Wang, A. E. Topolska, and R. L. Coppel.** 2005. MSP8 is a non-essential merozoite surface protein in *Plasmodium falciparum*. Mol. Biochem. Parasitol. **144:**27–35.
3. **Blackman, M. J., H. G. Heidrich, S. Donachie, J. S. McBride, and A. A. Holder.** 1990. A single fragment of a malaria merozoite surface protein remains on the parasite during red cell invasion and is the target of invasion-inhibiting antibodies. J. Exp. Med. **172:**379–382.
4. **Blackman, M. J., and A. A. Holder.** 1992. Secondary processing of the *Plasmodium falciparum* merozoite surface protein-1 (MSP1) by a calcium-dependent membrane-bound serine protease: shedding of MSP133 as a noncovalently associated complex with other fragments of the MSP1. Mol. Biochem. Parasitol. **50:**307–315.
5. **Blackman, M. J., T. J. Scott-Finnigan, S. Shai, and A. A. Holder.** 1994. Antibodies inhibit the protease-mediated processing of a malaria merozoite surface protein. J. Exp. Med. **180:**389–393.
6. **Bozdech, Z., M. Llinas, B. L. Pulliam, E. D. Wong, J. Zhu, and J. L. DeRisi.** 2003. The transcriptome of the intraerythrocytic developmental cycle of *Plasmodium falciparum*. PLoS Biol. **1:**E5.
7. **Drew, D. R., P. R. Sanders, and B. S. Crabb.** 2005. *Plasmodium falciparum* merozoite surface protein 8 is a ring-stage membrane protein that localizes to the parasitophorous vacuole of infected erythrocytes. Infect. Immun. **73:**3912–3922.
8. **Duraisingh, M. T., A. G. Maier, T. Triglia, and A. F. Cowman.** 2003. Erythrocyte-binding antigen 175 mediates invasion in *Plasmodium falciparum* utilizing sialic acid-dependent and -independent pathways. Proc. Natl. Acad. Sci. U. S. A. **100:**4796–4801.
9. **Duraisingh, M. T., T. Triglia, and A. F. Cowman.** 2002. Negative selection of *Plasmodium falciparum* reveals targeted gene deletion by double crossover recombination. Int. J. Parasitol. **32:**81–89.
10. **Flueck, C., G. Frank, T. Smith, A. Jafarshad, I. Nebie, S. B. Sirima, S. Olugbile, P. Alonso, M. Tanner, P. Druilhe, I. Felger, and G. Corradin.** 2009. Evaluation of two long synthetic merozoite surface protein 2 peptides as malaria vaccine candidates. Vaccine **27:**2653–2661.
11. **Gardner, M. J., N. Hall, E. Fung, O. White, M. Berriman, R. W. Hyman, J. M. Carlton, A. Pain, K. E. Nelson, S. Bowman, I. T. Paulsen, K. James, J. A. Eisen, K. Rutherford, S. L. Salzberg, A. Craig, S. Kyes, M. S. Chan, V. Nene, S. J. Shallom, B. Suh, J. Peterson, S. Angiuoli, M. Pertea, J. Allen, J. Selengut, D. Haft, M. W. Mather, A. B. Vaidya, D. M. Martin, A. H. Fairlamb, M. J. Fraunholz, D. S. Roos, S. A. Ralph, G. I. McFadden, L. M. Cummings, G. M. Subramanian, C. Mungall, J. C. Venter, D. J. Carucci, S. L. Hoffman, C. Newbold, R. W. Davis, C. M. Fraser, and B. Barrell.** 2002. Genome sequence of the human malaria parasite *Plasmodium falciparum*. Nature **419:**498–511.
12. **Genton, B., F. Al-Yaman, I. Betuela, R. F. Anders, A. Saul, K. Baea, M. Mellombo, J. Taraika, G. V. Brown, D. Pye, D. O. Irving, I. Felger, H. P. Beck, T. A. Smith, and M. P. Alpers.** 2003. Safety and immunogenicity of a three-component blood-stage malaria vaccine (MSP1, MSP2, RESA) against *Plasmodium falciparum* in Papua New Guinean children. Vaccine **22:**30–41.
13. **Gerold, P., L. Schofield, M. J. Blackman, A. A. Holder, and R. T. Schwarz.** 1996. Structural analysis of the glycosyl-phosphatidylinositol membrane anchor of the merozoite surface proteins-1 and -2 of *Plasmodium falciparum*. Mol. Biochem. Parasitol. **75:**131–143.
14. **Gilberger, T. W., J. K. Thompson, T. Triglia, R. T. Good, M. T. Duraisingh, and A. F. Cowman.** 2003. A novel erythrocyte binding antigen-175 paralogue from *Plasmodium falciparum* defines a new trypsin-resistant receptor on human erythrocytes. J. Biol. Chem. **278:**14480–14486.
15. **Good, M. F., D. C. Kaslow, and L. H. Miller.** 1998. Pathways and strategies for developing a malaria blood-stage vaccine. Annu. Rev. Immunol. **16:**57–87.
16. **Hall, N., M. Karras, J. D. Raine, J. M. Carlton, T. W. Kooij, M. Berriman, L. Florens, C. S. Janssen, A. Pain, G. K. Christophides, K. James, K. Rutherford, B. Harris, D. Harris, C. Churcher, M. A. Quail, D. Ormond, J. Doggett, H. E. Trueman, J. Mendoza, S. L. Bidwell, M. A. Rajandream, D. J. Carucci, J. R. Yates III, F. C. Kafatos, C. J. Janse, B. Barrell, C. M. Turner, A. P. Waters, and R. E. Sinden.** 2005. A comprehensive survey of the *Plasmodium* life cycle by genomic, transcriptomic, and proteomic analyses. Science **307:**82–86.
17. **Hisaeda, H., A. Saul, J. J. Reece, M. C. Kennedy, C. A. Long, L. H. Miller, and A. W. Stowers.** 2002. Merozoite surface protein 3 and protection against malaria in *Aotus nancymai* monkeys. J. Infect. Dis. **185:**657–664.
18. **Jouin, H., W. Daher, J. Khalife, I. Ricard, O. M. Puijalon, M. Capron, and D. Dive.** 2004. Double staining of *Plasmodium falciparum* nucleic acids with hydroethidine and thiazole orange for cell cycle stage analysis by flow cytometry. Cytometry A **57:**34–38.
19. **Kadekoppala, M., R. A. O'Donnell, M. Grainger, B. S. Crabb, and A. A. Holder.** 2008. Deletion of the *Plasmodium falciparum* merozoite surface protein 7 gene impairs parasite invasion of erythrocytes. Eukaryot. Cell **7:**2123–2132.
20. **Koussis, K., C. Withers-Martinez, S. Yeoh, M. Child, F. Hackett, E. Knuepfer, L. Juliano, U. Woehlbier, H. Bujard, and M. J. Blackman.** 2009. A multifunctional serine protease primes the malaria parasite for red blood cell invasion. EMBO J. **28:**725–735.
21. **Le Roch, K. G., J. R. Johnson, L. Florens, Y. Zhou, A. Santrosyan, M. Grainger, S. F. Yan, K. C. Williamson, A. A. Holder, D. J. Carucci, J. R. Yates III, and E. A. Winzeler.** 2004. Global analysis of transcript and protein levels across the *Plasmodium falciparum* life cycle. Genome Res. **14:**2308–2318.
22. **Le Roch, K. G., Y. Zhou, P. L. Blair, M. Grainger, J. K. Moch, J. D. Haynes, P. De La Vega, A. A. Holder, S. Batalov, D. J. Carucci, and E. A. Winzeler.** 2003. Discovery of gene function by expression profiling of the malaria parasite life cycle. Science **301:**1503–1508.
23. **Llinás, M., Z. Bozdech, E. D. Wong, A. T. Adai, and J. L. DeRisi.** 2006. Comparative whole genome transcriptome analysis of three *Plasmodium falciparum* strains. Nucleic Acids Res. **34:**1166–1173.
24. **Lusingu, J. P., S. Gesase, S. Msham, F. Francis, M. Lemnge, M. Seth, S. Sembuche, A. Rutta, D. Minja, M. D. Segeja, S. Bosomprah, S. Cousens, R. Noor, R. Chilengi, and P. Druilhe.** 2009. Satisfactory safety and immunogenicity of MSP3 malaria vaccine candidate in Tanzanian children aged 12–24 months. Malar. J. **8:**163.
25. **Mackinnon, M. J., J. Li, S. Mok, M. M. Kortok, K. Marsh, P. R. Preiser, and Z. Bozdech.** 2009. Comparative transcriptional and genomic analysis of *Plasmodium falciparum* field isolates. PLoS Pathog. **5:**e1000644.
26. **Maier, A. G., M. T. Duraisingh, J. C. Reeder, S. S. Patel, J. W. Kazura, P. A. Zimmerman, and A. F. Cowman.** 2003. *Plasmodium falciparum* erythrocyte invasion through glycophorin C and selection for Gerbich negativity in human populations. Nat. Med. **9:**87–92.
27. **Mair, G. R., J. A. Braks, L. S. Garver, J. C. Wiegant, N. Hall, R. W. Dirks, S. M. Khan, G. Dimopoulos, C. J. Janse, and A. P. Waters.** 2006. Regulation of sexual development of *Plasmodium* by translational repression. Science **313:**667–669.
28. **Mello, K., T. M. Daly, C. A. Long, J. M. Burns, and L. W. Bergman.** 2004. Members of the merozoite surface protein 7 family with similar expression patterns differ in ability to protect against *Plasmodium yoelii* malaria. Infect. Immun. **72:**1010–1018.
29. **Mello, K., T. M. Daly, J. Morrisey, A. B. Vaidya, C. A. Long, and L. W. Bergman.** 2002. A multigene family that interacts with the amino terminus of *Plasmodium* MSP-1 identified using the yeast two-hybrid system. Eukaryot. Cell **1:**915–925.
30. **Mills, K. E., J. A. Pearce, B. S. Crabb, and A. F. Cowman.** 2002. Truncation of merozoite surface protein 3 disrupts its trafficking and that of acidic-basic repeat protein to the surface of *Plasmodium falciparum* merozoites. Mol. Microbiol. **43:**1401–1411.
31. **Mongui, A., O. Perez-Leal, S. C. Soto, J. Cortes, and M. A. Patarroyo.** 2006. Cloning, expression, and characterisation of a *Plasmodium vivax* MSP7 family merozoite surface protein. Biochem. Biophys. Res. Commun. **351:**639–644.
32. **Nebie, I., A. Diarra, A. Ouedraogo, A. B. Tiono, A. T. Konate, A. Gansane, I. Soulama, S. Cousens, O. Leroy, and S. B. Sirima.** 2009. Humoral and cell-mediated immunity to MSP3 peptides in adults immunized with MSP3 in malaria endemic area, Burkina Faso. Parasite Immunol. **31:**474–480.
33. **Pachebat, J. A., M. Kadekoppala, M. Grainger, A. R. Dluzewski, R. S. Gunaratne, T. J. Scott-Finnigan, S. A. Ogun, I. T. Ling, L. H. Bannister, H. M. Taylor, G. H. Mitchell, and A. A. Holder.** 2007. Extensive proteolytic processing of the malaria parasite merozoite surface protein 7 during biosynthesis and parasite release from erythrocytes. Mol. Biochem. Parasitol. **151:**59–69.
34. **Pachebat, J. A., I. T. Ling, M. Grainger, C. Trucco, S. Howell, D. Fernandez-Reyes, R. Gunaratne, and A. A. Holder.** 2001. The 22 kDa component of the protein complex on the surface of *Plasmodium falciparum* merozoites is derived from a larger precursor, merozoite surface protein 7. Mol. Biochem. Parasitol. **117:**83–89.
35. **Pasvol, G., R. J. Wilson, M. E. Smalley, and J. Brown.** 1978. Separation of viable schizont-infected red cells of *Plasmodium falciparum* from human blood. Ann. Trop. Med. Parasitol. **72:**87–88.
36. **Pearce, J. A., K. Mills, T. Triglia, A. F. Cowman, and R. F. Anders.** 2005. Characterisation of two novel proteins from the asexual stage of *Plasmodium falciparum*, H101 and H103. Mol. Biochem. Parasitol. **139:**141–151.
37. **Persson, K. E., C. T. Lee, K. Marsh, and J. G. Beeson.** 2006. Development and optimization of high-throughput methods to measure *Plasmodium falciparum*-specific growth inhibitory antibodies. J. Clin. Microbiol. **44:**1665–1673.
38. **Reed, M. B., S. R. Caruana, A. H. Batchelor, J. K. Thompson, B. S. Crabb, and A. F. Cowman.** 2000. Targeted disruption of an erythrocyte binding antigen in *Plasmodium falciparum* is associated with a switch toward a sialic acid-independent pathway of invasion. Proc. Natl. Acad. Sci. U. S. A. **97:**7509–7514.
39. **Richards, J. S., and J. G. Beeson.** 2009. The future for blood-stage vaccines against malaria. Immunol. Cell Biol. **87:**377–390.
40. **Sanders, P. R., P. R. Gilson, G. T. Cantin, D. C. Greenbaum, T. Nebl, D. J.**

Carucci, M. J. McConville, L. Schofield, A. N. Hodder, J. R. Yates III, and B. S. Crabb. 2005. Distinct protein classes including novel merozoite surface antigens in Raft-like membranes of *Plasmodium falciparum*. J. Biol. Chem. **280:**40169–40176.

41. **Sanders, P. R., L. M. Kats, D. R. Drew, R. A. O'Donnell, M. O'Neill, A. G. Maier, R. L. Coppel, and B. S. Crabb.** 2006. A set of glycosylphosphatidyl inositol-anchored membrane proteins of *Plasmodium falciparum* is refractory to genetic deletion. Infect. Immun. **74:**4330–4338.
42. **Stafford, W. H., B. Gunder, A. Harris, H. G. Heidrich, A. A. Holder, and M. J. Blackman.** 1996. A 22 kDa protein associated with the *Plasmodium falciparum* merozoite surface protein-1 complex. Mol. Biochem. Parasitol. **80:**159–169.
43. **Stoute, J. A., and W. R. Ballou.** 1998. The current status of malaria vaccines. BioDrugs **10:**123–136.
44. **Taylor, H. M., M. Grainger, and A. A. Holder.** 2002. Variation in the expression of a *Plasmodium falciparum* protein family implicated in erythrocyte invasion. Infect. Immun. **70:**5779–5789.
45. **Tewari, R., S. A. Ogun, R. S. Gunaratne, A. Crisanti, and A. A. Holder.** 2005. Disruption of *Plasmodium berghei* merozoite surface protein 7 gene modulates parasite growth in vivo. Blood **105:**394–396.
46. **Triglia, T., M. T. Duraisingh, R. T. Good, and A. F. Cowman.** 2005. Reticulocyte-binding protein homologue 1 is required for sialic acid-dependent invasion into human erythrocytes by *Plasmodium falciparum*. Mol. Microbiol. **55:**162–174.
47. **Trucco, C., D. Fernandez-Reyes, S. Howell, W. H. Stafford, T. J. Scott-Finnigan, M. Grainger, S. A. Ogun, W. R. Taylor, and A. A. Holder.** 2001. The merozoite surface protein 6 gene codes for a 36 kDa protein associated with the *Plasmodium falciparum* merozoite surface protein-1 complex. Mol. Biochem. Parasitol. **112:**91–101.
48. **Wang, L., L. Crouch, T. L. Richie, D. H. Nhan, and R. L. Coppel.** 2003. Naturally acquired antibody responses to the components of the *Plasmodium falciparum* merozoite surface protein 1 complex. Parasite Immunol. **25:**403–412.